American Mineralogist, Volume 92, pages 1456–1463, 2007

Pressure-induced change in the compressional behavior of the O-H bond in chrysotile: A Raman high-pressure study up to 4.5 GPa

Tomoyuki Mizukami,[1,2,*] Hiroyuki Kagi,[1] Simon R. Wallis,[2] and Satoshi Fukura[1]

[1]Geochemical Laboratory, Graduate School of Science, University of Tokyo, Tokyo 113-0033, Japan
[2]Department of Earth and Planetary Science, Graduate School of Environmental Studies, Nagoya University, Nagoya 464-8602, Japan

Abstract

A change in the linear pressure behavior of the chrysotile Raman O-H band is revealed by an in-situ high-pressure Raman study using a diamond anvil cell (DAC) at 0.1–0.4 GPa pressure intervals. The peak of 3701 cm^{-1} can be accurately determined in the pressure range of 0.2–4.5 GPa regardless of peak fitting models. The pressure (P)-wavenumber (ν) relationship for the peak is closely approximated by two linear functions with the slopes ($d\nu/dP$) of 4.3 cm^{-1}/GPa and 1.7 cm^{-1}/GPa at pressures above and below 1.7 GPa, respectively. The spectral resolution given by a peak fitting method (0.5 cm^{-1}) implies that these functions for changes in the positions of the 3701 cm^{-1} peak provide pressure estimates with resolutions of 0.1–0.2 GPa. This method can be used to estimate remnant pressure in natural samples in the form of thin sections. The pressure shift characterized by the change in slope and the associated decrease of the peak width can be explained by a model where the change in compressibility of the tetrahedral layer affects the interaction between the inner O-H and Si atoms forming a six-membered ring. The high-pressure dependence at pressures lower than 1.7 GPa may be a contribution of a dominant layer-parallel (in-plane) compression that compensates a distortion in the tetrahedral layer of chrysotile. The conclusion that chrysotile changes its compressibility at around 1.7 GPa is significant for understanding of the properties of chrysotile nano-fibers and possibly for thermodynamic consideration on serpentine phase relations.

Keywords: High-pressure Raman spectroscopy, chrysotile, pressure scale, O-H bond, compressional behavior of sheet silicate

Introduction

Serpentine minerals are characterized by a 1:1 layer structure consisting of octahedral and tetrahedral sheets. The dimensional misfit between the sheets is compensated in several ways, leading to the principle polymorphs of serpentine: lizardite, antigorite, and chrysotile (Wicks and O'Hanley 1988). In contrast to the planar structures of lizardite and antigorite, chrysotile characteristically forms cylindrical fiber crystals that give the characteristic properties of asbestos. In addition to these varieties, transmission electron microscopy (TEM) and high-resolution TEM studies (Wicks and O'Hanley 1988; Baronnet and Devouard 1996; Dódony and Buseck 2004a) have revealed the existence of "polygonal serpentine;" a cylindrical polymorph with axis-parallel sectored structures. The properties of these cylindrical serpentines have been recently the subject of close study in part due to their potential industrial applications as nanoscale fiber structures (Falini et al. 2004; Mamontov et al. 2005).

The serpentine minerals are major constituents of hydrated upper mantle of oceanic plates (Muller et al. 1997) and the wedge mantle overlying subduction zones (Ulmer and Trommsdorff 1999; Bostock et al. 2002). They are considered to play a major role in the cycling of water and mobile elements in the upper mantle (Ulmer and Trommsdorff 1999; Rüpke et al. 2004) and in the tectonic and seismic processes (Freyer et al. 1985; Guillot et al. 2001; Dobson et al. 2002; Jung et al. 2004). The stability field of antigorite extends up to 650–700 °C and 5 GPa (Ulmer and Trommsdorff 1995; Wunder and Schreyer 1997; Bromiley and Pawley 2003) while lizardite and chrysotile are inferred to be stable at temperatures below 400 °C (Evans 2004). However, the low-temperature phase relations of lizardite and chrysotile are not well known (e.g., Ulmer and Trommsdorff 1999). The phase relations including the serpentine minerals are much less sensitive to pressure changes. For these reasons, it is difficult to use petrological analysis of serpentine minerals to estimate the depths at which the host rocks originated.

Laser Raman spectroscopy can detect vibrational modes of interatomic bonds in minerals varying with physical conditions such as temperature, pressure, and anisotropic stress. Well-known geological applications are estimations of fossil pressures in fluid and solid inclusions using the relative shifts of the Raman peak centers (Izraeli et al. 1999; Sobolev et al. 2000; Yamamoto et al. 2002; Zedgenizov et al. 2004). This method is potentially applicable to a wide range of rock-forming minerals (including serpentine minerals) provided that the relations between the Raman peak positions and pressure are accurately calibrated for the mineral of interest. In particular, pressure dependence of hydroxyl (O-H) stretching vibration can be a sensitive indicator

* E-mail: miz@nagoya-u.jp

for the pressure-response of hydrogen bonds in hydrous minerals (e.g., Komatsu et al. 2005).

Raman spectra of serpentine minerals consist of O-H stretching regions (3600–3800 cm^{-1}, at ambient pressure) and the low frequency regions related to the metal-oxygen bonds (Kloprogge et al. 1999; Auzende et al. 2004). Auzende et al. (2004) carried out a high-pressure Raman study of serpentine minerals using a diamond anvil cell (DAC). These authors show that the Raman peaks of the four serpentine polymorphs shift positively with increasing pressure up to 10 GPa. They regard the peak positions to change continuously and linearly with pressure and suggest that serpentine minerals do not undergo any phase transition in the pressure range. However, the pressure resolution of the experiment of Auzende et al. (2004) is insufficient especially at pressures lower than 3 GPa and cannot exclude the possibility of a structural change. The recent high-pressure studies of a 1:1 layer silicate, dickite (Johnston et al. 2002; Dera et al. 2003), and a high-resolution TEM study of lizardite (Dódony and Buseck 2004b) pointed out the existence of polytypism or transformation controlled by pressure.

Considering the geological occurrence of chrysotile, detailed pressure calibration is more important at such lower pressures. By combining the high temperature limit of 400 °C (Evans 2004) with the geotherms numerically calculated for the coolest conditions of subduction boundaries (Peacock 1996), a high-pressure limit of the stability of chrysotile is found to be lower than 2.3–2.5 GPa. Most of chrysotile generally occurs in near surface environments (Evans 2004).

The aims of this study are (1) to examine the shifts of Raman peaks for chrysotile and (2) to determine the relations between the peak shifts and pressure accurately enough for geological use. For these purposes in-situ high-pressure Raman measurements using a DAC were carried out from 0.2 to 4.5 GPa. We show that the pressure shift of the chrysotile O-H peak (3701 cm^{-1}) includes a change in dv/dP slope at around 1.7 GPa. Based on this result we briefly discuss the crystallographic implications of the pressure behavior and present the pressure-wavenumber relation of the chrysotile O-H peak as a new pressure scale.

Experimental procedures

Raman analysis

Raman measurements were carried out using the micro-Raman system at Geochemical Laboratory, University of Tokyo. Ar^+ laser operated at 514.5 nm by an air-cooled ion laser source (Melles Griot) is guided through an optical fiber into an optical microscope (Olympus, BX60) and is focused on samples mounted on the stage using objective lenses. The 20× objective lens (Olympus, LM Plan FI, 20× N.A. = 0.40) is used for in-situ measurement in a DAC. In this system the output power of 100 mW produces an irradiation power of 20 mW on the samples. Scattered light is collected in a back-scattered geometry with a holographic supernotch plus filter (Kaiser, HSPF-514.5-1.0) that effectively attenuates the Rayleigh line. Polarization directions of incident and scattered lights are not controlled. Raman spectra are acquired with a single polychrome spectrograph (Chromex, 250is) equipped with a charge-coupled-device (CCD) detector (Andor, DU420-OE) of 1024 × 128 pixels. The wavenumber resolution of the spectrograph is approximately 1 cm^{-1} per pixel in the range of 2970–4000 cm^{-1} using a 1800 lines/mm grating. The width of the entrance slit is 50 μm. This gives Raman spectra with the maximum spectral resolution and sufficient signal intensity.

The spectrograph is calibrated for each Raman measurement using an O-H stretching band of synthetic brucite at 3650.0 cm^{-1}, and a peak of naphthalene at 3056.4 cm^{-1}. For this frequency calibration the positions of the reference peaks are calculated using a curve fitting program installed in the "GRAMS" software. In the present study, O-H stretching modes of the sample were analyzed very carefully to detect subtle changes induced by pressure. Recently, Fukura et al. (2006) revealed that considerable changes due to thermal expansion of the CCD occur during the initial stages of measurement. We paid great attention to ensure that the system was stabilized before data acquisition.

DAC experiment

The high-pressure experiments were conducted in a DAC equipped with a pair of type Ib diamonds with a 600 μm diameter culet. Samples and a ruby chip are set within a 300 μm diameter hole drilled in a 250 μm thick alloy "Inconel 750" gasket. The extra space is filled with a 4:1 methanol-ethanol mixture to achieve quasi-hydrostatic pressure through uniaxial loading of the diamonds. Pressure is determined by the shift of the R_1 fluorescence peak of ruby (Piermarini et al. 1975) compared to the atmospheric peak position. Precision in the pressure determination is less than 0.1 GPa. Raman spectra are measured under quasi-stable pressures with the maximum deviation of 5%.

Sample description

The sample of chrysotile used in this study was collected from the Higashi-akaishi peridotite body in the Sanbagawa metamorphic belt, SW Japan (Mizukami and Wallis 2005). It occurs as a vein material along a fracture in serpentinized peridotite in the form of bundles of straight fiber crystals with a pale yellowish-green color. The fibers show a parallel alignment oblique to the fracture plane, indicating that the growth of chrysotile was associated with opening and displacement. X-ray diffraction analysis indicates that the sample is probably chrysotile rather than lizardite and antigorite. The decrease of refractive index at pressures as high as 6 GPa (invisible in the alcohol pressure medium) is more a distinct identification of chrysotile and can distinguish it from polygonal serpentine (Auzende et al. 2004).

Results

O-H Raman spectra of chrysotile

The Raman O-H stretching bands of chrysotile serpentine were monitored on compression and subsequent decompression at room temperature. After several experimental runs we obtained a series of the Raman spectra for the O-H stretching region at pressure conditions up to 4.5 GPa with intervals of 0.1–0.4 GPa. Selected Raman spectra of the wavenumber range of 3550–3800 cm^{-1} are shown in Figure 1. Raman intensities are normalized by the maximum intensity of each spectrum. The Raman band due to the O-H group in chrysotile mainly consists of a strong peak at 3701 cm^{-1} with a shoulder around 3690 cm^{-1}. A peak with a minor intensity is observed at 3650 cm^{-1}.

The major band at around 3690–3700 cm^{-1} shifts toward higher wavenumbers as pressure increases. In the experimental pressure range the peak originally at 3701 cm^{-1} shows a distinct shape that narrows slightly at higher pressures. With increasing pressures the shoulder at 3690 cm^{-1} seems to gradually decrease its intensity relative to the 3701 cm^{-1} peak and, instead, a broad peak enlarges at the higher frequency side of the 3701 cm^{-1} peak (on the right side in Fig. 1). The minor peak of 3650 cm^{-1} is apparently broadened in the higher pressures and becomes inconspicuous due to the relatively low S/N ratios of the Raman spectra at higher pressures. The general trend of the spectral change upon compression is consistent with the result of Auzende et al. (2004). A very similar spectroscopic behavior was observed for chlorite up to 9 GPa by Kleppe et al. (2003).

Peak fit calculation

The O-H Raman spectra of chrysotile can be modeled with a combination of several peaks. An important step to establish a Raman pressure scale is to find the most reliable peak whose position can be determined with sufficient precision and reproducibility. We evaluated two models for resolving the O-H band of chrysotile: (1) four-peak model and (2) five-peak model (Fig. 2). Both models are based on the idea that the ambient spectra of the O-H band of chrysotile are fitted by four peaks of pseudo-Voigt functions (Kloprogge et al. 1999). The four-peak model (model 1) assumes that the shift of the 3687 cm^{-1} peak (ν3) overtakes that of the higher one (3701 cm^{-1}, ν4) as pressure increases. Auzende et al. (2004) propose that these groups of O-H peaks can be assigned to the outer O-H group and inner O-H group, respectively. On the other hand, the five-peak model (model 2) assumes that a peak (ν3') on the high frequency side of the 3701 cm^{-1} peak (ν4) gradually strengthens its signal intensity with increasing pressures and that the shoulder formed by 3683 and 3690 cm^{-1} peaks (ν2 and ν3) simply diminishes. Comparable changes of Raman O-H bands are observed in brucite at high pressure (Duffy et al. 1995).

Peak fitting calculation used the GRAMS software package, and peak shapes were modeled by the pseudo-Voigt function. The fitting parameters (FWHM, Gaussian/Lorentzian mixing parameter and peak positions) were not constrained during the iteration unless the resultant values are significantly different from those obtained at the final pressure conditions. A high Gaussian component of the pseudo-Voigt function (>0.9) is only assumed to be intrinsic for the sharp peak of 3701 cm^{-1} in the pressure range of this study because it is clearly shown by the low pressure spectra (Fig. 1). We accept the results of iteration with an R^2 value higher than 0.95.

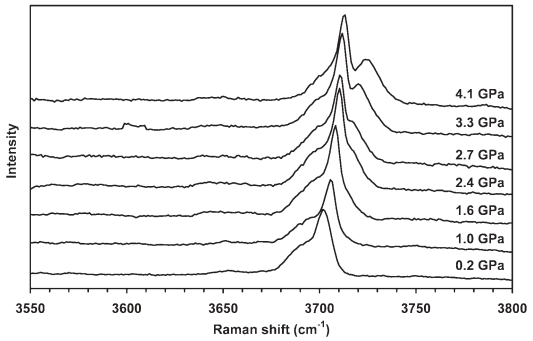

FIGURE 1. Selected Raman O-H spectra of chrysotile. Pressure conditions are shown at the right of the spectra. As pressure increases a sharp peak at 3701 cm^{-1} slightly shifts to high wavenumber and a broad band grows at the high frequency side of the 3701 cm^{-1} peak.

The results of the peak fitting analysis are shown in Figure 3. The position of the 3701 cm^{-1} peak (ν4) is determined with a precision (1σ) of 0.1 cm^{-1}, regardless of the fitting models (Fig. 3 and Table 1). In contrast, larger uncertainties are involved in determination of the positions of other peaks (0.4–3.3 cm^{-1} at 1σ level).

Wavenumbers of the peak centers of the O-H Raman band generally increased with compression. The results for ν4 and ν3' apparently trace continuous pressure shifts (Figs. 3a and 3b). The pressure vs. wavenumber relations of ν2 and ν3 are discontinuous for model 1 (Fig. 3a), reflecting a difficulty in fitting the positions of two closely overlapping peaks. The influence of such artifacts is relatively small in model 2 (Fig. 3b). Nonetheless, the fact that two models give an almost identical result for the pressure-wavenumber relation of the 3701 cm^{-1} peak (ν4) (Fig. 3) suggests that this peak is effectively independent of the model used to fit the spectra.

Pressure behavior of chrysotile O-H band

A change in linear pressure behavior of the chrysotile O-H band is clearly shown by the pressure vs. wavenumber profile of ν4 (Fig. 3c), in which the slope $\Delta\nu/\Delta P$ at high pressure conditions is smaller than that at lower pressures. Figure 4a shows $\Delta\nu/\Delta P$ values at experimental conditions calculated by linear least-squares fitting for three neighboring data (Fig. 4a). Calculated $\Delta\nu/\Delta P$ is almost constant (4.2 ± 0.5 cm^{-1}/GPa) at 0.4–1.6 GPa and it shows lower values that can be approximated by 1.9 ± 1.1 cm^{-1}/GPa at 1.8–4.5 GPa. The change of $\Delta\nu/\Delta P$ probably takes place at a pressure range of 1.6–1.8 GPa, although relatively large errors in the peak positions induce a large deviation in $\Delta\nu/\Delta P$ at this pressure range.

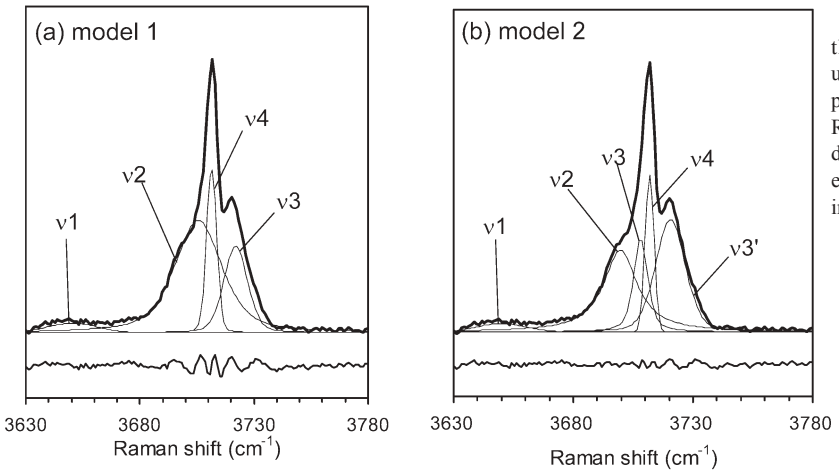

FIGURE 2. Peak fitting models for the chrysotile O-H band. (**a**) Model 1 uses four peaks and (**b**) model 2 uses five peaks to the Raman spectrum at 3.3 GPa. Raw data of Raman spectra (bold line), deconvolution curves (thin line), and residual errors (lowermost line) are shown in relative intensity.

TABLE 1. Fit parameters for pressure-wavenumber relations of the chrysotile O-H peaks in this study

Peak no. (ν_0)	1σ (ν) (Min–Max)	ν_0 (cm^{-1})	0–1.7 GPa dν/dP (cm^{-1}/GPa)	R^2	ν_0 (cm^{-1})	1.7–4.5 GPa dν/dP (cm^{-1}/GPa)	R^2
Model 1							
ν1 (3650)	–	–	–	–	–	–	–
ν2 (3683)	0.8 (0.1–2.5)	3679.9	9.4	0.758	3684.3	5.4	0.741
ν3 (3690)	0.5 (0–1.5)	3686.6	13.1	0.857	3692.8	8.1	0.933
ν4 (3701)	0.1 (0–0.2)	3701.4	4.2	0.994	3706.0	1.6	0.932
Model 2							
ν1 (3650)	–	–	–	–	–	–	–
ν2 (3683)	3.3 (0.3–5.6)	3683.0	5.3	0.683	3684.5	4.3	0.764
ν3 (3690)	0.8 (0.1–2.0)	3689.5	8.6	0.837	3698.5	2.7	0.566
ν4 (3701)	0.1 (0–0.5)	3701.3	4.3	0.998	3706.0	1.7	0.903
ν3′ (3714)	0.4 (0.1–1.1)	3712.8	1.2*	0.441	3707.9	4.0	0.951

* 0.4–1.7 GPa for ν3′.

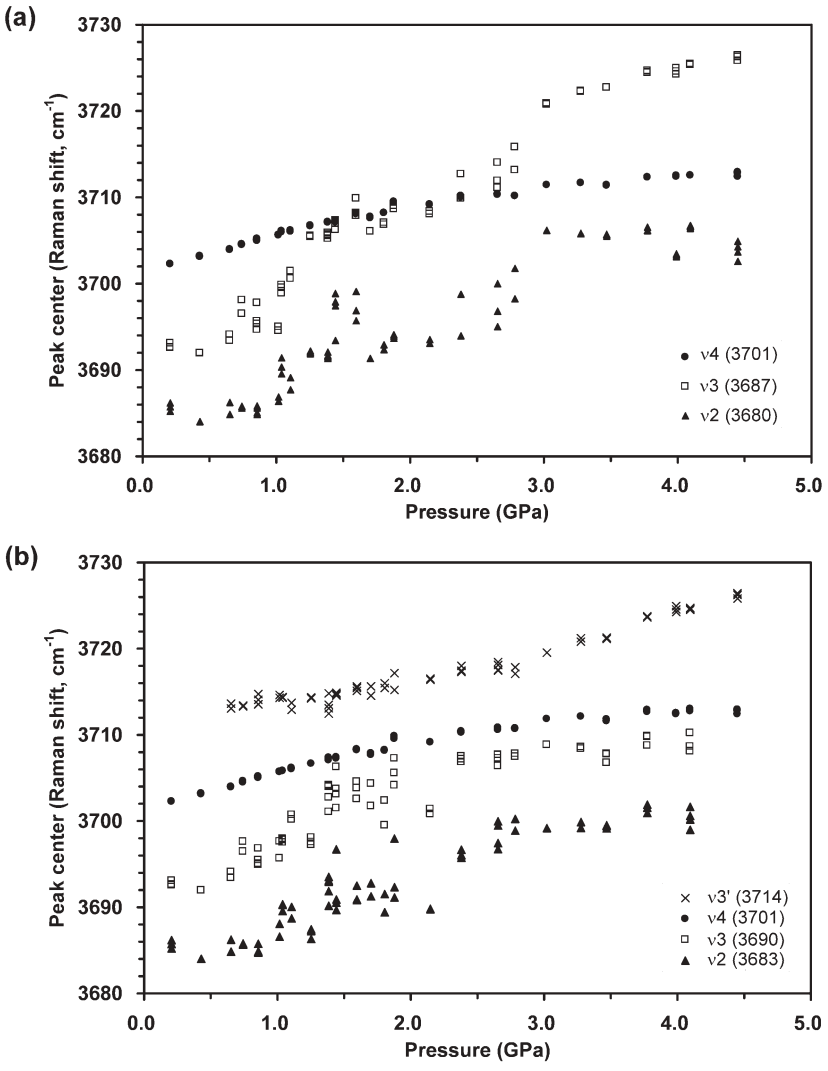

FIGURE 3. Peak centers of the Raman O-H peaks at various pressure conditions. They are determined by peak fitting calculations based on (**a**) model 1 and (**b**) model 2.

Recognition of two constant slopes shows that the pressure-wavenumber relation of ν4 cannot be modeled by a single linear relationship. We suggest that the relationship can be described by a combination of two linear functions (Fig. 4b). The parameters of the linear least-squares fit for the experimental results are listed in Table 1, and indicate good correlations for these linear fits. The high values of correlation coefficients ($R^2 > 0.9$) show good correlations of these linear fittings. The pressure coefficient dν/dP for the peak ν4 is 4.2 cm^{-1}/GPa at 0–1.7 GPa and 1.7 cm^{-1}/GPa at 1.7–4.5 GPa. These values of dν/dP are significantly different from the previously proposed value (2.4 cm^{-1}/GPa) based on an assumption of a single linear ν-P relation

(Auzende et al. 2004), which results in a pressure overestimate of 1.2 GPa (70 rel%) in maximum.

Discussion

Proposal of a Raman geobarometer: Pressure-wavenumber relation for the chrysotile 3701 cm^{-1} peak

The results of high-pressure Raman spectroscopy of chrysotile and spectral deconvolution show that the position of the peak 3701 cm^{-1} (ν4) can be determined with a deviation of less than 0.4 cm^{-1} (1σ) at pressures of 0.2–4.5 GPa. The pressure-wavenumber relation of ν4 is closely approximated by the following two linear equations corresponding to lower and higher pressure ranges:

$$P = (\nu - 3701.3)/4.3 \text{ for } \nu \leq 3709.1 \text{ (low } P\text{)} \quad (1a)$$

$$P = (\nu - 3706.0)/1.7 \text{ for } \nu > 3709.1 \text{ (high } P\text{)} \quad (1b)$$

where ν (cm^{-1}) is the wavenumber of the center of the ν4 Raman peak and P (GPa) is pressure. The position of the peak center is determined using a model where the O-H stretching modes of Raman spectrum are expressed as a combination of five pseudo-Voigt functions (model 2 in Fig. 2). ν is given as the peak center of the fourth pseudo-Voigt function in order of wavenumber. It should be noted that the peak fitting model is simply an empirical approximation and is not based on any reliable theory.

The above equations for the peak ν4 are based on close correlations to precisely determined experimental data so that the pressure shift of this peak can be used as a quantitative pressure scale (i.e., geobarometer). The fit for Equation 1a is particularly good with a correlation coefficient (R^2) exceeding 0.99 (Table 1). Pressure resolutions of this new pressure scale practically depend on the wavenumber resolutions of peak center determination. Our results show that the position of the peak 3701 cm^{-1} (ν4) can be determined with deviation lower than 0.4 cm^{-1} (1σ) at pressures of 0.2–4.5 GPa. If a wavenumber resolution of 0.4 cm^{-1} is associated with determination of a Raman peak center, the corresponding pressure resolutions are ±0.1 GPa and ±0.2 GPa for Equations 1a and 1b, respectively.

The precise determination of ν4 peak center position is important for application of the geobarometer using the chrysotile Raman O-H band, which will require a wavenumber resolution lower than spectral resolutions of spectrographs (generally above 1 cm^{-1}). Such apparent high resolutions can be attained by a peak fitting calculation that gives the best curve for numerous points in a wavenumber-intensity coordinate (Izraeli et al. 1999; Fukura et al. 2006). For example, the spectral resolution of the Raman system in Geochemical Laboratory, University of Tokyo, is ±0.05 cm^{-1} (Fukura et al. 2006). This value corresponds to the amplitude of wavenumber fluctuation due to room temperature variation (±0.4 °C) after the CCD detector is fully stabilized. In addition, checking the wavenumber distance from a position of chrysotile ν4 peak at ambient pressure is effective in reducing deviations caused by wavenumber calibration.

Chrysotile crystals are found enclosed in olivine, pyroxenes, and spinel group minerals in a wide range of ultramafic rocks. The bulk modulus of chrysotile is significantly lower than these host minerals described above (Holland and Powell 1998) and, therefore, residual pressures are likely to be generated in such inclusions of chrysotile. Our proposed geobarometer can estimate these pressures from samples of thin section.

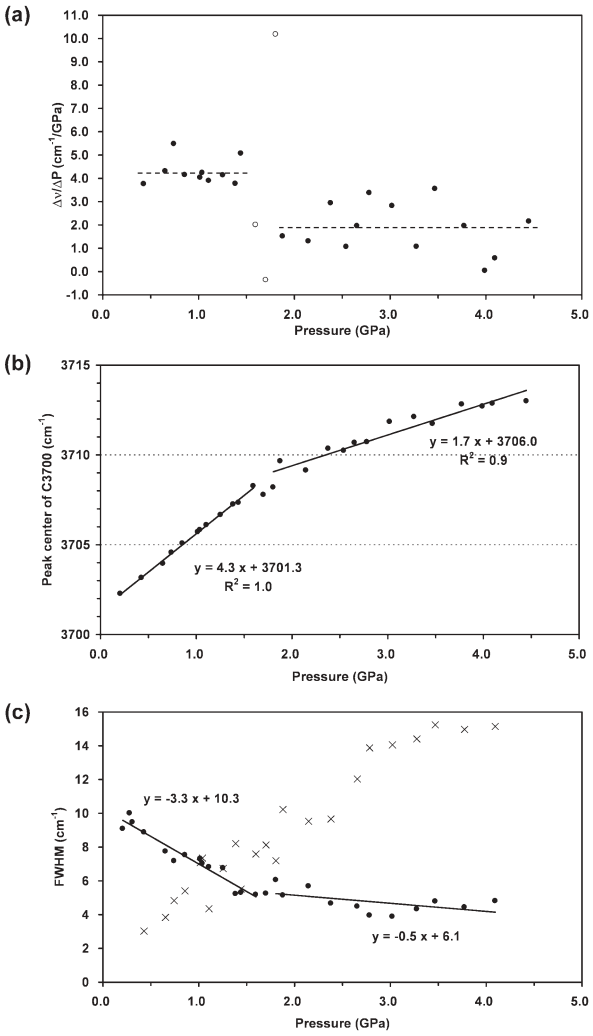

Figure 4. (**a**) Δν/ΔP of the 3701 cm^{-1} peak (model 2) calculated from linear least-square fit of three neighboring (P, ν) data sets. Dashed lines indicate the averages of Δν/ΔP values at lower and higher pressure conditions (4.2 and 1.9 cm^{-1}/GPa, respectively). Open circles denote data not counted in Δν/ΔP averages (see text). (**b**) Pressure-wavenumber relation for the 3701 cm^{-1} peak centers (model 2) and results of linear least-square fit calculation. (**c**) Full width half maximum (FWHM) of the 3701 cm^{-1} peak (solid circle) and 3714 cm^{-1} peak (cross) at pressure conditions of 0.2–4.5 GPa.

Significance of the change in linear behavior of the chrysotile O-H band

O-H stretching bands in layered silicates and other hydrous minerals are strongly affected by the compressional behavior of the atomic interactions around the O-H bonds. Our observations reveal two distinct positive linear trends with changing pressure. This result has significant mineralogical implications for the compressional behavior of the chrysotile crystal structure and

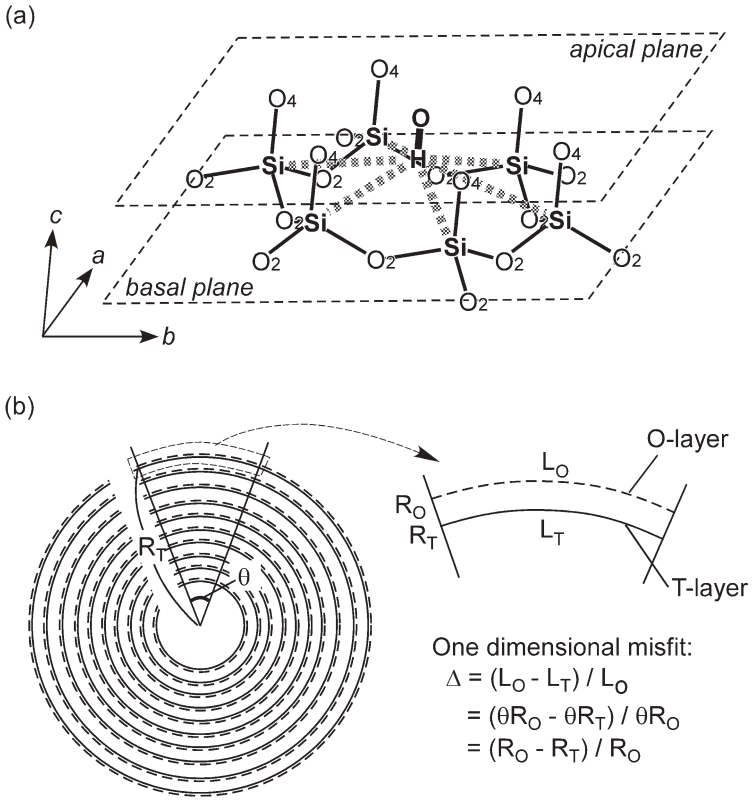

FIGURE 5. (**a**) Silicon-proton interactions in the tetrahedral layer of chrysotile. This schematic diagram is based on the atomic positions of lizardite 1T (Mellini and Zanazzi 1987). The apical plane includes O4 and O(H) oxygen atoms and the basal plane includes O2. (**b**) Schematic diagram of chrysotile structure illustrating the lateral misfit between the octahedral layer (O-layer, broken line) and the tetrahedral layer (T-layer, solid line). R is the radius of a tubular layer and L is its segment with a central angle θ. One dimensional lateral misfit, Δ, is defined by $(L_O - L_T)/L_O$. Δ is likely to be consistent with crystallographic misfit at the innermost sheet and decreases with a radius of sheet (R_O). If a layer distance, $R_O - R_T$, is constant, the distances among basal oxygen atoms should be stretched in the outer tetrahedral layers.

for the assignments of the Raman spectra to the O-H bonds. In the literature, both positive and negative pressure dependences are reported for the Raman O-H bands of hydrous minerals (e.g., Duffy et al. 1995; Hofmeister et al. 1999; Kleppe et al. 2003; Liu et al. 2003; Kawamoto et al. 2004; Komatsu et al. 2005). The positive shifts are attributed to (1) O-H compression or (2) weakening of hydrogen bonds due to lengthening of the distances and changes of O-H···O angles (e.g., Liu et al. 2003). The negative shifts of O-H bands are characteristically observed for hydroxides (e.g., Duffy et al. 1995) and liquid water (e.g., Kawamoto et al. 2004; Okada et al. 2005) in which the hydrogen bonds effectively weaken the O-H bonds. In general, the pressure dependence is determined by some balance between these two effects: O-H compression and hydrogen bond.

Serpentine minerals have two types of O-H bonds in the tri-octahedral 1:1 layer structures: inner O-H and outer O-H. Auzende et al. (2004) suggest that the relatively weak pressure dependence of the 3701 cm^{-1} peak likely corresponds to the inner O-H at the middle of 1:1 layer structure. Our experimental results show additional evidence in support of this suggestion. The dν/dP value at pressures above 1.7 GPa (1.7 cm^{-1}/GPa) is close to that of talc O-H peak (1.3 cm^{-1}/GPa, unpublished data), implying that the atomic structure around the corresponding inner O-H bond of chrysotile has changed to be almost identical to that around the intralayer O-H bond of talc. The decrease of the peak width at higher pressure conditions (Fig. 4c) is also consistent with inner O-H surrounded by six-membered rings in the tetrahedral sheet. In contrast, the Raman signals arising from the outer O-H are expected to be more sensitive to pressure than those from the inner O-H because the compaction is dominant in interlayer space (Auzende et al. 2004). Stacking of curved layers causes a positional disorder of O-H···O angles resulting in a broad O-H band (Kloprogge et al. 1999). Layer-parallel displacement that is probably associated with axial compaction of the chrysotile tube may enhance broadening of the band. These features that are expected to occur for the outer O-H bands are clearly observed in the spectral behavior of the 3714 cm^{-1} peak (Figs. 3 and 4c).

Based on the assumption that the Raman peak initially at 3701 cm^{-1} represents the vibrational mode of the inner O-H, we discuss an atomic interpretation for the change in the linear positive profile of the chrysotile 3701 cm^{-1} peak with decrease of dν/dP (Fig. 4). The importance of the cation-proton interactions is suggested from the high-pressure Raman studies of the tri-octahedral and di-octahedral 2:1 layer aluminosilicates (Holtz et al. 1993) and clinochlore (Kleppe et al. 2003). Cation-proton Coulombic repulsion in the tri-octahedral layer stiffens the intralayer O-H bonds resulting in a positive shift of the O-H band. Similarly the positive shift of chrysotile 3701 cm^{-1} can be explained by O-H compression due to the interaction with Si atoms consisting of a six-membered ring in the chrysotile tetrahedral sheet (Fig. 5a). Considering that the sudden decrease of dν/dP at around 1.7 GPa indicates a change in the compressibility of the O-H bond, we conclude that the chrysotile tetrahedral sheet changes its mode of compression with a smaller increment of the O-H···Si interaction.

A possible explanation for the change of compressibility is that at lower pressures, a shortening of the tetrahedral sheet is

dominant in layer-parallel (in-plane) rather than layer-normal direction and at a critical pressure (around 1.7 GPa), the Si-O bond lengths of tetrahedra become almost identical among apical O and basal O resulting in a lower rate of Si-O shortening. The structure refinements of lizardite (Mellini and Zanazzi 1987) provide an estimate of the flattening of Si-O tetrahedra (2–5% shorter in the apical Si-O). Cylindrically stacking layers of chrysotile show various radii exceeding the ideal one (calculated to be at 88 Å by Whittaker 1957) suggesting the misfit between the octahedral and tetrahedral layers is not compensated by the curvature (Wicks and O'Hanley 1988) (Fig. 5b). In the 1:1 layers of the larger radii (i.e., outer sheets), the tetrahedral layers are considered to be under tensional stresses (Wicks and O'Hanley 1988). In contrast, the Raman peak arising from the intralayer O-H bond of talc, in which the Si-O bond lengths are equal in the tetrahedral layer (Rayner and Brown 1973), shows a linear pressure dependence (Holtz et al. 1993).

At pressures higher than 1.7 GPa, at which tetrahedra in the chysotile tetrahedral layer probably have attained regular Si-O bonds, chrysotile is considered to follow the mode of compression observed in talc. Upon compression, talc mainly reduces the thickness of the tetrahedral layer by shortening of the apical Si-O bonds of the tetrahedra (Stixrude 2002). The layer-parallel compression of the talc tetrahedral layer is less dominant and is accommodated by tetrahedral rotation (Stixrude 2002). A similar anisotropic compaction is observed by the high pressure X-ray study of clinochlore (Welch and Marshall 2001). This compressional mechanism may be less effective in increasing the O-H···Si interaction than layer-parallel shortening. This can explain the smaller positive dν/dP value of the chrysotile 3701 cm^{-1} peak above 1.7 GPa (Fig. 4).

At present, considering that the atomic positions of H and the details of O-H···O interactions in serpentine minerals are not clarified by a high-pressure diffraction study, we cannot completely exclude possible effects of hydrogen bonding. Therefore, there is still room for other explanations of the observed change in dν/dP slope based on another band assignment of the 3701 cm^{-1} peak (Kloprogge et al. 1999) or a transformation due to O-H bending (Pellenq et al. 2005). Comparison with the high-pressure behavior of O-H bands in antigorite and lizardite will be good verification of whether the change in linear behavior in the pressure range of 0–4.5 GPa is peculiar to chrysotile or common to serpentine minerals, and will help remove ambiguity in the interpretation. In either crystallographic model the observed change of the dν/dP slope is best interpreted as a sign that the compressibility of chrysotile decreases at around 2 GPa. This pressure behavior is directly related to the physical property (cf. layer curvature) of chrysotile fiber and may influence phase relations. Further detailed examinations of the atomic behavior of chrysotile are required to fully document the change in the linear behavior of this mineral which is important in both mineralogy and nanotechnology.

Acknowledgments

We thank M. Welch and E. Reusser for their detailed comments that helped refine the manuscript. This work was supported by a Grant-in-Aid for Scientific Research (15340190, 18654098, 18340177) from the Japan Society for Promotion of Science (JSPS) and by a Grant-in-aid for The 21st Century COE Program for Frontiers in Fundamental Chemistry from the Ministry of Education, Culture, Sports, Science and Technology. H.K. is grateful for Grant-in-Aid from Sumitomo Foundation and Inamori Foundation. T.M. acknowledges the financial support of a JSPS Research Fellowship for Young Scientists. With great regret, we announce that since this study was completed our coauthor, Satoshi Fukura, has passed away; a tragic loss to us and to his field of a young researcher full of promise for the future.

References cited

Auzende, A-L., Daniel, I., Reynard, B., and Lemaire, C. (2004) High-pressure behaviour of serpentine minerals: a Raman spectroscopic study. Physics and Chemistry of Minerals, 31, 269–277.

Baronnet, A. and Devouard, B. (1996) Topology and crystal growth of natural chrysotile and polygonal serpentine. Journal of Crystal Growth, 166, 952–960.

Bostock, M.G., Hyndman, R.D., Rondenay, S., and Peacock, S.M. (2002) An inverted continental Moho and serpentinization of the forearc mantle. Nature, 417, 536–538.

Bromiley, G.D. and Pawley, A.R. (2003) The stability of antigorite in the systems MgO-SiO_2-H_2O (MSH) and MgO-Al_2O_3-SiO_2-H_2O (MASH): The effects of Al^{3+} substitution on high-pressure stability. American Mineralogist, 88, 99–108.

Dera, P., Prewitt, C.T., Japel, S., Bish, L.D., and Johnston, C.T. (2003) Pressure-controlled polytypism in hydrous layered materials. American Mineralogist, 88, 1428–1435.

Dobson, D.P., Meredith, P.G., and Boon, S.A. (2002) Simulation of subduction zone seismicity by dehydration of serpentine. Science, 298, 1407–1410.

Dódony, I. and Buseck, P.R. (2004a) Serpentine close-up and intimate: An HRTEM view. International Geology Review, 46, 507–527.

——— (2004b) Lizardite-chlorite structural relationships and an inferred high-pressure lizardite polytype. American Mineralogist, 89, 1631–1639.

Duffy, T.S., Meade, C., Fei, Y., Mao, H.-K., and Hemley, R.J. (1995) High-pressure phase transition in brucite, $Mg(OH)_2$. American Mineralogist, 80, 222–230.

Evans, B.W. (2004) The serpentine multisystem revisited: Chrysotile is metastable. International Geology Review, 46, 479–506.

Falini, G., Foresti, E., Gazzano, M., Gualtieri, A.F., Leoni, M., Lesci, I.G., and Roveri, N. (2004) Tubular-shaped stoichiometric chrysotile nanocrystals. Chemistry, 10, 3043–3049.

Freyer, P., Ambos, E.L., and Hussong, D.M. (1985) Origin and emplacement of Mariana forearc seamounts. Geology, 13, 774–777.

Fukura, S., Mizukami, T., Odake, S., and Kagi, H. (2006) Factors determining the stability, resolution, and precision of a conventional Raman spectrometer. Applied Spectroscopy, 60, 946–950.

Guillot, S., Hattori, K.H., de Sigoyer, J., Ngler, T., and Auzende A.-L. (2001) Evidence of hydration of the mantle wedge and its role in the exhumation of eclogites. Earth and Planetary Science Letters, 193, 115–127.

Hofmeister, A.M., Cynn, H., Burnley, P.C., and Meade, C. (1999) Vibrational spectra of dense, hydrous magnesium silicates at high pressure: Importance of the hydrogen bond angle. American Mineralogist, 84, 454–464.

Holland, T.J.B. and Powell, R. (1998) An internally consistent thermodynamic data set for phases of petrological interest. Journal of Metamorphic Geology, 16, 309–343.

Holtz, M., Solin, S.A., and Pinnavaia, T.J. (1993) Effect of pressure on the Raman vibrational modes of layered aluminosilicate compounds. Physical Review B, 48, 13312–13317.

Izraeli, E.S., Harris, J.W., and Navon, O. (1999) Raman barometry of diamond formation. Earth and Planetary Science Letters, 173, 351–360.

Johnston, C.T., Wang, S-L., Bish, D.L., Dera, P., Agnew, S.F., and Kenney, J.W. III. (2002) Novel pressure-induced phase transformations in hydrous layered materials. Geophysical Research Letters, 29, DOI: 10.1029/2002GL015402.

Jung, H.-Y., Green II, H.W., and Dobrzhinetskaya, L.F. (2004) Intermediate-depth earthquake faulting by dehydration embrittlement with negative volume change. Nature, 428, 545–549.

Kawamoto, T., Ochiai, S., and Kagi, H. (2004) Changes in the structure of water deduced from the pressure dependence of the Raman OH frequency. Journal of Chemical Physics, 120, 5867–5870.

Kleppe, A.L., Jephcoat, A.P., and Welch, M.D. (2003) The effect of pressure upon hydrogen bonding in chlorite: a Raman spectroscopic study of clinochlore to 26.5 GPa. American Mineralogist, 88, 567–573.

Kloprogge, J.T., Frost, R.L., and Rintoul, L. (1999) Single crystal Raman microscopic study of the asbestos mineral chrysotile. Physical Chemistry Chemical Physics, 1, 2559–2564.

Komatsu, K., Kagi, H., Okada, T., Kuribayashi, T., Parise, J.B., and Kudoh, Y. (2005) Pressure dependence of OH stretching mode in F-rich natural topaz and topaz-OH. American Mineralogist, 90, 266–270.

Liu, Z.-X., Lager, G.A., Hemley, R.J., and Ross, N.L. (2003) Synchrotron infrared spectroscopy of OH-chondrodite and OH-clinohumite at high pressure. American Mineralogist, 88, 1412–1415.

Mamontov, E., Kumzerov, Y.A., and Vakhrushev, S.B. (2005) Translational dynamics of water in the nanochannels of oriented chrysotile asbestos fibers. Physical Review E, 71, 061502.

Mellini, M. and Zanazzi, P.F. (1987) Crystal structures of lizardite 1T and lizardite-2H1 from Coli, Italy. American Mineralogist, 72, 943–948.
Mizukami, T. and Wallis, S.R. (2005) Structural and petrological constraints on the tectonic evolution of the garnet-lherzolite facies Higashi-akaishi peridotite body, Sanbagawa belt, SW Japan. Tectonics, 24, TC6012, DOI: 10.1029/2004TC001733.
Muller, M.R., Robinson, C.J., Minshull, T.A., White, R.S., and Bickle, M.J. (1997) Thin crust beneath ocean drilling program borehole 735B at the Southwest Indian Ridge? Earth and Planetary Science Letters, 148, 93–107.
Okada, T., Komatsu, K., Kawamoto, T., Yamanaka, T., and Kagi, H. (2005) Pressure response of Raman spectra of water and its implication to the change in hydrogen bond interactions. Spectrochimica Acta A, 61, 2423–2427.
Peacock, S.M. (1996) Thermal and petrologic structure of subduction zones. AGU Geophysical Monograph, 96, 119–133.
Pellenq, R.J., Auzende, A., Devouard, B., Baronnet, A., and Grauby, O. (2005) Free energy minimization calculations of lizardite at variable pressures and temperatures. Abstract. AGU Fall Meeting, EOS Transaction, 86.
Piermarini, G.L., Block, S., Barnett, J.D., and Forman, R.A. (1975) Calibration of the pressure dependence of the R1 ruby fluorescence line to 195 kbar. Journal of Applied Physics, 46, 2774–2780.
Rayner, J.H. and Brown, G. (1973) The crystal structure of talc. Clays and Clay Minerals, 21, 103–114.
Rüpke, L.H., Morgan, J.P., Hort, M., and Connolly, J.A.D. (2004) Serpentine and the subduction zone water cycle. Earth and Planetary Science Letters, 223, 17–34.
Stixrude, L. (2002) Talc under tension and compression: Spinodal instability, elasticity, and structure. Journal of Geophysical Research, 107(B12), 2327, DOI: 10.1029/2001JB001684.
Sobolev, N.V., Fursenko, B.A., Goryainov, S.V., Shu, J., Hemley, R.J., Mao, H.-K., and Boyd, F.R. (2000) Fossilized high pressure from the Earth's deep interior: The coesite-in-diamond barometer. Geology, 97, 11875–11879.
Ulmer, P. and Trommsdorff, V. (1995) Serpentine stability to mantle depths and subduction-related magmatism. Science, 268, 858–861.
——— (1999) Phase relations of hydrous mantle subducting to 300 km. In Y. Fei, C.M. Bertka, and B.O. Mysen, Eds., Mantle petrology: Field observations and high pressure experimentation, 6, p. 259–281. Geochemical Society Special Publication, The Geochemical Society, Houston, Texas.
Welch, M.D. and Marshall, W.G. (2001) High-pressure behavior of clinochlore. American Mineralogist, 86, 1380–1386.
Whittaker, E.J.W. (1957) The structure of chrysotile. V. Diffuse reflections and fibre texture. Acta Crystallographica, 10, 149.
Wicks, F.J. and O'Hanley, D.S. (1988) Serpentine minerals: structures and petrology. In S.W. Bailey, Ed., Hydrous phyllosilicates, 19, p. 91–167. Reviews in Mineralogy, Mineralogical Society of America, Chantilly, Virginia.
Wunder, B. and Schreyer, W. (1997) Antigorite: High-pressure stability in the system MgO-SiO_2-H_2O (MSH). Lithos, 41, 213–227.
Yamamoto, J., Kagi, H., Kaneoka, I., Lai, Y., Prikhod'ko, V.S., and Arai, S. (2002) Fossil pressures of fluid inclusions in mantle xenoliths exhibiting rheology of mantle minerals using micro-Raman spectroscopy. Earth and Planetary Science Letters, 198, 511–519.
Zedgenizov, D.A., Kagi, H., Shatsky, V.S., and Sobolev, N.V. (2004) Carbonatitic melts in cuboid diamonds from Udachnaya kimberlite pipe (Yakutia): evidence from vibrational spectroscopy. Mineralogical Magazine, 68, 61–73.

Manuscript received October 26, 2006
Manuscript accepted April 13, 2007
Manuscript handled by Martin Kunz